



Article

An Efficient Pilot Assignment Scheme for Addressing Pilot Contamination in Multicell Massive MIMO Systems

Ahmed S. Al-hubaishi ^{1,*}, Nor Kamariah Noordin ^{1,2}, Aduwati Sali ^{1,2}, Shamala Subramaniam ^{3,4} and Ali Mohammed Mansoor ⁵

¹ Department of Computer and Communication Engineering, Universiti Putra Malaysia, Serdang 43400, Malaysia; nknordin@upm.my (N.K.N.); aduwati@upm.edu.my (A.S.)

² Wireless and Photonics Networks Laboratory, Universiti Putra Malaysia, Serdang 43400, Malaysia

³ Department of Communication Technology and Network, Universiti Putra Malaysia, Serdang 43400, Malaysia; drshamala@gmail.com

⁴ Sports Academy, Universiti Putra Malaysia, Serdang 43400, Malaysia

⁵ Faculty of Computer Science & Information Technology, University of Malaya, Kuala Lumpur 50603, Malaysia; ali.mansoor@um.edu.my

* Correspondence: alhubaishiahmed033@gmail.com; Tel.: +60-967-777-888-129

Received: 25 February 2019; Accepted: 21 March 2019; Published: 27 March 2019



Abstract: The reuse of the same pilot group across cells to address bandwidth limitations in a network has resulted in pilot contamination. This causes severe inter-cell interference at the targeted cell. Pilot contamination is associated with multicell massive multiple-input multiple-output (MIMO) systems which degrades the system performance even when extra arrays of antennas are added to the network. In this paper, we propose an efficient pilot assignment (EPA) scheme to address this issue by maximizing the minimum uplink rate of the target cell's users. To achieve this, we exploit the large-scale characteristics of the fading channel to minimize the amount of outgoing inter-cell interference at the target cell. Results from the simulation show that the EPA scheme outperforms both the conventional and the smart pilot assignment (SPA) schemes by reducing the effect of inter-cell interference. These results, show that the EPA scheme has significantly improved the system performance in terms of achievable uplink rate and cumulative distribution function (CDF) for both signal-to-interference-plus-noise ratio (SINR), and uplink rate.

Keywords: pilot contamination; massive MIMO; pilot assignment; large-scale fading coefficients

1. Introduction

Equipping the base station (BS) with a large number of antennas (also known as massive multiple-input multiple-output (MIMO)) has been considered one of the fundamental technologies that leads to 5G [1]. The introduction of this technology is to meet the increasing demand for mobile data in 5G [2]. Although the use of massive MIMO systems increases spectral efficiency, enhances energy efficiency, and reduces the effect of small scale fading [3–7], but invariably promotes pilot contamination. In massive MIMO, time-division duplex (TDD) protocol is preferred over the frequency-division duplex (FDD) [8,9], as the former allows channel estimation in one direction (i.e., uplink) and avoids the estimation of the other side (i.e., downlink) due to channel reciprocity property. In other words, the use of TDD

based channel reciprocal minimizes the overhead signals used for channel estimation, which largely saves network bandwidth. Although, the channel estimation ensures high utilization of TDD massive MIMO via uplink transmission, but its channel coherence blocks are restricted in size (limited size). Therefore, the orthogonal pilot sequences cannot be allocated for all users among the cells. To overcome this problem, the orthogonal pilot sequences have to be reused across the cells. Although, pilot reuse approach is a remarkable way forward in addressing the associated problem, however, the channel estimate obtained in a given cell will be contaminated by pilots transmitted by users in other cells. Specifically, the inter-cell interference exacerbates the estimation error and also makes sure the channel estimation of two or more users sharing the same pilot sequence is correlated at a given cell [10]. Thus, with multicell massive MIMO systems, its performance deteriorates during uplink and downlink transmission. This issue is referred to as pilot contamination, and depicted in Figure 1.

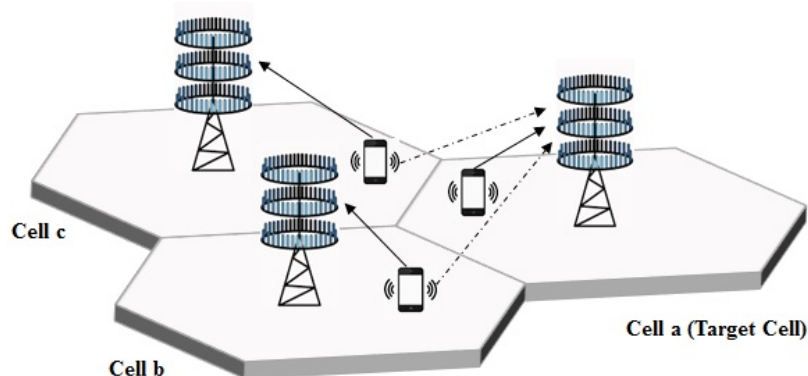


Figure 1. The effect of pilot contamination in multicell massive MIMO systems at a cell *a*, where the solid line represents the direct gain and the dotted line represents the inter-cell interference.

To address the issue associated with pilot contamination, several research methods have been proposed to eliminate/relieve pilot contamination. Among these methods, the pilot assignment technique is identified to be a potential technique for solving this problem. Smart pilot assignment (SPA) method proposed by [11], focused on adjusting the combination between the users and pilot sequences, but did not consider inter-cell interference which causes the pilot contamination. In this paper, we propose an efficient pilot assignment mechanism to improve the performance of users with respect to intense pilot contamination in multicell massive MIMO systems. We summarize our contributions below:

- We formulate the pilot assignment as an optimization problem and develop a heuristic algorithm, in order to maximize the minimum throughput considering the reduction in the inter-cell interference pilot contamination.
- We evaluate the performance of the proposed mechanism in terms of signal-to-interference-plus-noise ratio (SINR), and uplink rate with an extensive MATLAB simulation.
- We compare our work with SPA and other conventional schemes.

The rest of this paper is organized as follows. The related work is summarized in Section 2, the system model is described in Section 3, the pilot contamination phenomenon and the achievable uplink rate are illustrated in Section 4, the EPA scheme is explained in Section 5, the simulation results are depicted in Section 6, and finally, this paper is concluded in Section 7.

Notation: Throughout this paper, the bold lower case letters represent vectors and matrices are represented by bold upper case letters. \mathbf{I}_M denotes the identity matrix of dimensions $M \times M$. The operators $(\cdot)^{-1}$, $(\cdot)^T$, and $(\cdot)^H$ are defined for inverse, transpose and conjugate transpose operations, respectively. The expectation operator is represented by $E[\cdot]$.

2. Related Work

Different traditional algorithms based on pilot assignment have been proposed for pilot decontamination [12,13]. A vertex graph-coloring-based pilot assignment has been proposed in [12], the pilot sequences are allocated to the users according to the inter-cell interference (ICI) graph. The evaluation of ICI graph depends on both angle of arrival (AoA) correlation and distances between users. However, this scheme requires a second order channel information to construct ICI graph. A deep learning-based pilot allocation scheme (DL-PAS) is proposed in [13] to address the pilot contamination problem in massive MIMO systems. This algorithm aims at learning from the relationship between pilot assignment and users' location. However, the DL algorithm requires high data and subsequently takes a longer time to process the data.

The authors in [14,15] developed the location-based pilot assignment approaches for pilot decontamination. A new expression for line of sight (LOS) interference is derived in [14] which is considered as the criteria for pilot allocation. Although, there was an improvement in the sum spectral efficiency (SE), but the pilot assignment process takes a longer time to be implemented, especially in large networks. The work in [15] characterizes the angular region of the targeted user, and the pilot assignment process was implemented with the aim of making this region interference-free. This angular region is characterized by both the number of BS antennas and the location of the targeted user. However, the pilot assignment problem is formulated by the joint optimization problems which subsequently introduce high computational complexity.

In [16,17], the pilot allocation based pilot reuse (reuse factor more than 1) is also considered for pilot contamination's elimination technique. A systematically-constructed pilot reuse method is proposed in [16]. In this approach, the neighbor cells are allowed to use different sets of pilot sequences according to the tree division. To improve performance, it ensures larger distance between cells that share similar pilot sets, the depth of the tree is increased as the pilot contamination severity increases. This approach offers an effective performance when the ratio of the channel coherence time to the number of users in each cell is relatively large. For the purpose of improving the quality of service (QoS) of the edge users, a soft pilot reuse (SPR) scheme was proposed by [17]. The channel quality for each user is initially compared with a determined threshold before the pilot allocation procedure, but an increase in complexity was recorded due to additional computational cost incurred by finding the optimal threshold value.

By considering a fairness among users in order to mitigate the pilot contamination, pilot allocation schemes were proposed in [18,19]. Specifically, to maximize the sum rate of the system and guarantee fairness among users, a pilot allocation scheme was proposed by [18]. An optimization problem is formulated based on a max-product criterion, then both min-leakage algorithm and user-exchange algorithm based on greedy (UEBG) pilot allocation were suggested to solve the optimization problem. Although this scheme almost achieves the same performance as the optimal exhaustive search algorithm (ESA), it still suffers a setback due to high complexity. For the purpose of pilot contamination mitigation in [19], the pilot assignment scheme based on the harmonic SINR utility function was introduced to regulate the fairness among users. However, the system complexity increases as the number of users and network size grows (more than two cells).

Based on performance degradation of users, a pilot assignment scheme has been proposed in [20], the degradation performance is initially evaluated for all users according to the value of the uplink achievable rate. Therefore, the optimal pilot sequences were assigned to users who suffered from the highest degradation in a greedy way. Obviously, this scheme is not effective in bad channel conditions.

In [11,21], the pilot allocation approaches aim at enhancing the performance of users who suffer from bad SINR. The pilot allocation in [21] focused on maximizing the sum capacity of the whole system for pilot decontamination. In this work, the pilot sequences were assigned initially to the users who have bad

channel condition. However, the complexity of the pilot assignment procedure increases as the network size is increased. A SPA scheme is proposed in [11] to improve the performance of users with poor SINR. Users with low channel quality were assigned to pilot sequences which resulted in a low interference. However, the achievement of this scheme is limited as it did not consider inter-cell interference which causes the pilot contamination.

Some authors have tried to make a combination of two schemes to get an improved performance as shown in [22,23]. As such, a joint pilot assignment scheme has been proposed by [22], in which time-shifted [24] and the SPA [11] schemes were combined in order to mitigate the effect of pilot contamination. Inter-group interference is suppressed according to [24] strategy, whereas SPA is used to reduce intra-group interference. Although an improved overall performance was recorded, the mutual interference between downlink data and uplink pilot signals cannot be eliminated despite the use of SPA scheme. New pilot assignment schemes such as greedy-based and swapping-based were implemented together with pilot contamination precoding design (PCP) for massive MIMO downlinks [23]. This combination offers a considerable improvement over the random pilot assignment, but the PCP matrix is changed according to the update in pilot assignment information.

By exploiting the channel sparsity for wideband massive MIMO system, the pilot contamination can be removed with the help of pilot assignment policy in [25]. The pilot assignment policy is designed to help identify the subspace of the desired channel. The difficulty in this approach, lies on how to deal with the subspace estimation, which can be realized through multiple frames after randomizing the pilot contamination.

Differing from the aforementioned works [11,20], we consider the source of inter-cell interference throughout pilot assignment, which is essentially the cause of the pilot contamination. In some other works [12–15], the availability of some factors (e.g., user location, AoA, or LOS interference) are needed for pilot assignment which are not always easy to estimate, while our approach requires only large-scale fading coefficients, which can be tracked easily as they do not frequently change during coherence interval. Besides, comparing to previous works [17–19,21], our algorithm is not computationally intensive, and therefore it can be applied for large-scale networks.

3. System Model

In this section, we describe the system model under which the TDD-massive MIMO systems are implemented. In this model, the uplink comprises L cells, in which each cell contains a BS equipped with M antennas. Furthermore, in each cell coverage area K single-antenna users communicate simultaneously to their designated BS, assuming that $M \gg K$ [2,5]. The propagation channels connecting the k -th user located in the j -th cell to the BS in i -th cell is modeled as Rayleigh block fading [26] and the channel vector $\mathbf{h}_{jk}^i \in \mathbb{C}^{M \times 1}$ is denoted as:

$$\mathbf{h}_{jk}^i = \mathbf{g}_{jk}^i \sqrt{\beta_{jk}^i} \tag{1}$$

where \mathbf{g}_{jk}^i and β_{jk}^i denote the small scale-fading vector and large-scale fading coefficient, respectively. The small scale-fading vector has a complex Gaussian distribution with zero mean and unity variance, $\mathcal{CN}(0, \mathbf{I}_M)$, while the large-scale fading coefficient is referred to the effect of both path-loss and shadowing and it can be tracked easily as it changes slowly during coherence interval $\tau_c = B_c T_c$ [27–29]. We use B_c and T_c to denote the coherence bandwidth and the coherence time, respectively. Figure 2 illustrates the coherence block for TDD protocol. We also consider that large-scale fading coefficient is equal for all antenna elements, assuming that the distance between user k and BS is significantly larger than the distances between antenna elements.

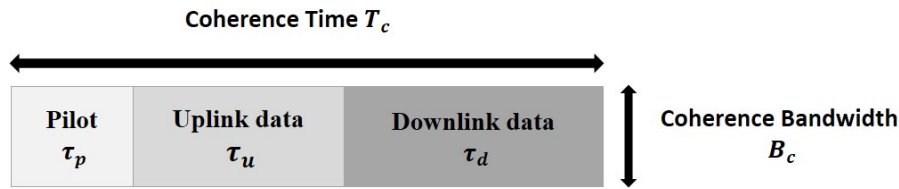


Figure 2. Time-division duplex (TDD) Protocol.

4. Pilot Contamination and Achievable Uplink Rate

Since the size of channel coherence blocks is limited, it is difficult to assign orthogonal pilot sequences to all users in order to prevent pilot contamination. Thus, it is necessary to reuse the pilot sequences in all cells to overcome this limitation [2]. The pilot sequences $\Phi = [\phi_1, \phi_2, \dots, \phi_K]^T \in \mathbb{C}^{M \times \tau_p}$ are assumed mutually orthogonal $\Phi^T \Phi = \tau_p \mathbf{I}_K$ with length of τ_p . During the pilot phase, the pilot sequences are distributed randomly to all users. Thus, the received signal $\mathbf{U}_i^\phi \in \mathbb{C}^{M \times \tau_p}$ at the BS in the i -th cell can be written as:

$$\mathbf{U}_i^\phi = \sqrt{\rho_\phi} \sum_{j=1}^L \sum_{k=1}^K \mathbf{h}_{jk}^i \phi_k^T + \mathbf{N}_i^\phi \tag{2}$$

$$\mathbf{U}_i^\phi = \sqrt{\rho_\phi} \sum_{k=1}^{K_i} \mathbf{h}_{ik}^i \phi_k^T + \sqrt{\rho_\phi} \sum_{\substack{j=1 \\ j \neq i}}^L \sum_{k=1}^{K_j} \mathbf{h}_{jk}^i \phi_k^T + \mathbf{N}_i^\phi \tag{3}$$

where ρ_ϕ denotes the pilot transmission power, and $\mathbf{N}_i^\phi \in \mathbb{C}^{M \times \tau_p}$ denotes the additive white Gaussian noise (AWGN) matrix which is assumed independent and identically distributed (i.i.d) random variables whose elements have zero mean and variance σ_N^2 . The received signal \mathbf{U}_i^ϕ is called the observation, in which the BS in the cell i can use it to estimate the channel responses. The first term in (3) represents the received pilot signals from users in the serving cell, whereas, the middle term represents the inter-cell interference signal from the neighbor cells, which causes the pilot contamination. Correspondingly, the received uplink data $\mathbf{u}_i^d \in \mathbb{C}^M$ at the BS in the i -th cell can be represented by:

$$\mathbf{u}_i^d = \sqrt{\rho_u} \sum_{j=1}^L \sum_{k=1}^K \mathbf{h}_{jk}^i x_{jk}^u + \mathbf{n}_i^u \tag{4}$$

where x_{jk}^u denotes the uplink transmitted symbol from user k located in the j -th cell, ρ_u denotes the power of the uplink transmitted symbol with $E[|x_{jk}^u|^2] = 1$, and $\mathbf{n}_i^u \in \mathbb{C}^{M \times \tau_u}$ denotes the AWGN vector with variance σ_n^2 and zero mean value. The minimum mean square error (MMSE) is exploited for the purpose of the channel estimation $\hat{\mathbf{h}}_{jk}^i \in \mathbb{C}^{M \times 1}$ [9]. Therefore, the MMSE estimated channel vector $\hat{\mathbf{h}}_{jk}^i$ based on the observation \mathbf{U}_i^ϕ in (2) can be given as [10]:

$$\hat{\mathbf{h}}_{jk}^i = \sqrt{\rho_u} \mathbf{R}_{jk}^i \boldsymbol{\Psi}_{jk}^i \mathbf{u}_{ijk}^p \tag{5}$$

and

$$\boldsymbol{\Psi}_{jk}^i = \left(\sum_{j,k} \rho_u \tau_p \mathbf{R}_{jk}^i + \sigma_u^2 \mathbf{I}_K \right)^{-1} \tag{6}$$

where $\mathbf{u}_{ijk}^p = \mathbf{U}_i^\phi \phi_k^*$ which is called the received proceed signal, $\mathbf{\Psi}_{jk}^i$ denotes the inverse of the normalized correlation matrix, and \mathbf{R}_{jk}^i denotes the spatial correlation matrix of the channel to be estimated, $\mathbf{R}_{jk}^i = E[\mathbf{h}_{jk}^i \mathbf{h}_{jk}^{iH}]$.

The estimated channel is then used to detect the uplink data symbol and precode the downlink data. Herein, we consider both maximum ratio combining (MRC) and zero forcing (ZF) as a linear detectors at the BS which are given by [30]:

$$\mathbf{A}_i = \begin{cases} \hat{\mathbf{H}}_i^i & \text{MRC} \\ \hat{\mathbf{H}}_i^i (\hat{\mathbf{H}}_i^{iH} \hat{\mathbf{H}}_i^i)^{-1} & \text{ZF} \end{cases} \quad (7)$$

The received detected signal is evaluated by multiplying the received uplink data signal \mathbf{u}_i^d by the decoding vector \mathbf{a}_{ik}^{iH} , which represents the k -th column of the matrix \mathbf{A}_i and \mathbf{h}_{ik}^i is the k -th column of the matrix \mathbf{H}_i^i . Therefore, the detected symbol of user k at a given BS located in a cell i can be expressed as:

$$z_{iik}^u = \mathbf{a}_{ik}^{iH} \mathbf{u}_i^d = \mathbf{a}_{ik}^{iH} \left(\sqrt{\rho_u} \sum_{j=1}^L \sum_{k=1}^K \mathbf{h}_{jk}^i x_{jk}^u + \mathbf{n}_i^u \right) \quad (8)$$

$$z_{iik}^u = \sqrt{\rho_u} \mathbf{a}_{ik}^{iH} \mathbf{h}_{ik}^i x_{ik}^u + \sqrt{\rho_u} \sum_{\substack{n=1 \\ n \neq k}}^{K_i} \mathbf{a}_{ik}^{iH} \mathbf{h}_{in}^i x_{in}^u + \sqrt{\rho_u} \sum_{\substack{j=1 \\ j \neq i}}^L \sum_{k=1}^{K_j} \mathbf{a}_{ik}^{iH} \mathbf{h}_{jk}^i x_{jk}^u + \mathbf{a}_{ik}^{iH} \mathbf{n}_i^u \quad (9)$$

The first term in (9) represents the desired signal, the second one represents the intra-cell interference, the third term is the effect of pilot contamination (inter-cell interference), and the last one represents the uncorrelated noise.

Consequently, the average SINR of the k -th user in the target cell i can be evaluated as:

$$SINR_{ik}^u = \frac{\rho_u |\mathbf{a}_{ik}^{iH} \mathbf{h}_{ik}^i|^2}{\rho_u \sum_{\substack{j=1 \\ j \neq i}}^L \sum_{k=1}^{K_j} |\mathbf{a}_{ik}^{iH} \mathbf{h}_{jk}^i|^2 + \frac{v_{ik}^i}{\rho_u}} \quad (10)$$

and

$$v_{ik}^i = \rho_u^2 \sum_{\substack{n=1 \\ n \neq k}}^{K_i} |\mathbf{a}_{ik}^{iH} \mathbf{h}_{in}^i|^2 + \rho_u \|\mathbf{a}_{ik}^i\|^2$$

where v_{ik}^i denotes the intra-cell interference and uncorrelated noise, in which their effect is almost neglected as the number of antennas increases ($M \rightarrow \infty$) [5]. Then, the uplink SINR can be described by large-scale fading coefficients β_{jk}^i as follows:

$$SINR_{ik}^u = \frac{\beta_{ik}^i{}^2}{\sum_{j \neq i} \beta_{jk}^i{}^2}, \quad \text{when } (M \rightarrow \infty) \quad (11)$$

It is clear from the above expression that the effect of small-scale fading and thermal noise are averaged out as the number of antennas is increased [5]. Therefore, the ergodic achievable uplink rate of the user k according to [26] is:

$$R_{ik}^u = \frac{1}{T_c} \sum_{\tau_u} (1 + SINR_{ik}^u) \quad (12)$$

where R_{jk}^u is calculated in bit/channel use and τ_u refers to the uplink duration. From (12), it is obvious that the average uplink rate of multicell massive MIMO systems is limited due to pilot contamination and it cannot be boosted by increasing either the number of serving antennas or both ρ_u and ρ_p .

5. Proposed Scheme

In this section, an efficient heuristic algorithm is developed for addressing the multicell massive MIMO associated problem. To do this, the assignment and the reuse of pilot group across cells in the network is formulated as an optimization problem.

5.1. Problem Formulation

Formally, we formulate an optimization problem as depicted in:

$$\mathcal{P} \xrightarrow{M \rightarrow \infty} \hat{\mathcal{P}} : \max_{\forall k \in i} \left(\min_{\forall \phi_k} \frac{\beta_{ik}^i{}^2}{\sum_{j \neq i} \beta_{jk}^i{}^2} \right) \quad (13)$$

The above optimization problem is based on the method proposed by [11]. In this method, it is assumed the number of antennas is very large and as such make use of the large-scale fading coefficients β_{jk}^i . To address problems related to pilot contamination, this study concentrates on assigning the pilot sequences for a specific cell in multicell massive MIMO systems. In the target cell, the number of possible iterations is defined by the number of K users which is usually very high. In contrast, the conventional scheme assigns the pilot sequences $\Phi = [\phi_1, \phi_2, \dots, \phi_K]^T$ randomly to K users.

The performance of multicell massive MIMO systems is much degraded by the effect of the strong inter-cell interference from the neighbor cells and is exacerbated when the channel quality of the users in target cell is poor. Specifically, in the SPA scheme, the set of users with the worst channel quality are assigned pilot sequences with the lowest inter-cell interference. Although these pilot sequences have the lowest interference, they are still considered high interference pilot sequences when used by users which have bad channel quality. Therefore, the interference that is associated with such pilot sequences must be minimized.

5.2. Proposed Solution

To achieve minimal outgoing inter-cell interference among neighbor cells for the target cell, we ensure a weak channel cross gain of the interfering users against desired users. The large-scale fading coefficients are used to measure the effect of inter-cell interference at the target BS. Thus, the effect of inter-cell interference can be measured by using these fading coefficients as it changes progressively during the coherence interval τ_c , as every user measured result is sent to its corresponding BS. The required conditions for finding the large-scale fading coefficients can be met in long term evolution-advanced (LTE-A) systems. These corresponding BSs contain the channel's information for the available BSs. The user keeps tracking these BSs until a reliable BS is identified for suitable handover. To enhance the cooperation among the BSs, we assume acquisition of the coordinated multi points (CoMP). Furthermore, a mobility management entity (MME) is connected to BSs by S1 interface and has a huge ability for computing. As a result, this unit can collect the large-scale fading coefficients from the connected BSs [31,32].

To abate the effect of setback suffered by users due to poor channel quality or high interference, the SINR is optimized. This is done by assigning the pilot sequence, which is associated with low interference, to users having poor channel quality.

In order to achieve this, we propose a heuristic algorithm based on SPA to solve the optimization problem in (13). Before illustrating the algorithm, we need to define a set of parameters η_{jk} which characterizes the squared cross gain of the interfering users from neighboring cells:

$$\eta_{jk} = \beta_{jk}^i{}^2, \quad k = 1, 2, \dots, K, \quad j = 1, 2, \dots, L \text{ and } j \neq i$$

The interference that is produced by users who shared the same pilot sequence ϕ_k can be evaluated at the target cell as:

$$\xi_k = \sum_{j \neq i} \eta_{jk} \tag{14}$$

In addition, the set of parameters ω_k is used to characterize the square channel quality of the target cell's users which can be expressed by:

$$\omega_k = \beta_{ik}^i{}^2, \quad k=1,2,\dots,K$$

So, the optimization problem in (13) can be re-written as the following:

$$\mathcal{P} \xrightarrow{M \rightarrow \infty} \hat{\mathcal{P}} : \max_{\forall k \in i} \left(\min_{\forall \phi_k} \frac{\omega_k}{\sum_{j \neq i} \eta_{jk}} \right) \tag{15}$$

The proposed algorithm EPA is summarized in Algorithm 1 to solve the above optimization problem.

Algorithm 1 Efficient Pilot Assignment (EPA).

- 1: **Input:**
 - 2: $\beta_{jk}^i \forall i, j \text{ and } k$
 - 3: **Output:**
 - 4: Assigning pilot sequences Φ for all users in all j cells $\forall j = 1, 2, \dots, L$
 - 5: **Procedure:**
for each neighbor cells $j \neq i$ do
for all users K in cell j do
 - 6: Evaluate: $\eta_{jk} = \beta_{jk}^i{}^2, k = 1, 2, \dots, K$
end for
 - 7: Classifying the users into different levels: $V_1, V_2, \dots, V_k, \dots, V_K$.
 $V_k = [\eta_{1k}, \eta_{2k}, \dots, \eta_{jk}, \dots, \eta_{(L-1)k}]$
 - 8: Assign the pilot sequence ϕ_k to the users in V_k .
end for
 - 9: Find the sum: $\xi_k = \sum_{j \neq i} \eta_{jk}, \xi_k \in [\xi_1, \xi_2, \dots, \xi_K] \forall \Phi$
for each user in the target cell i do
 - 10: Evaluate $\omega_k = \beta_{ik}^i{}^2, k = 1, 2, \dots, K$
end for
 - 11: Sort ω_k in descending order: $\omega_1 \geq \omega_2, \dots, \geq \omega_k, \dots, \geq \omega_K$
 - 12: Sort ξ_k in descending order: $\xi_1 \geq \xi_2 \geq, \dots, \geq \xi_k, \dots, \geq \xi_K$
 - 13: Assigning the pilot sequence ϕ_k , which associates with ξ_k , to the user who has ω_k .
-

The available large scale fading coefficients are exploited to measure the interference from the neighbor cells. From the above algorithm, the users in the neighbor cells are classified into different levels according to the value of squared cross gain (η_{jk}), which gives an indication of the strength of the interference at the target cell i . The users that cause the highest interference (which have the largest η_{jk}) are classified as the level V_1 users. This level involves the worst interfering users from each neighbor cell. The second level V_2 contains the users which cause less interference than that in V_1 . This classification process will continue until the last level V_K , which contains the users that produce the smallest interference. The k -th interference level can be represented by:

$$V_k = [\eta_{1k}, \eta_{2k}, \dots, \eta_{(L-1)k}] \tag{16}$$

The amount of interference that is produced by the users in each level is described by (14). After that, the interfering users in each level are assigned the same pilot sequence. For instance, the users in V_1 and V_K are assigned the pilot sequences ϕ_1 and ϕ_K , respectively. As a result, the pilot sequence ϕ_1 is suffering from the highest interference, whereas ϕ_K is the one with the lowest interference. The remaining pilot sequences have different levels of interference between ϕ_1 and ϕ_K . After minimizing the inter-cell interference at the serving BS, the second step is to assign pilot sequences to its users and this can be achieved by solving the following formula:

$$\mathcal{P} \xrightarrow{M \rightarrow \infty} \hat{\mathcal{P}} : \max_{\forall k \in i} \left(\min \frac{\omega_k}{\xi_k} \right) \tag{17}$$

Obviously, from the EPA algorithm, the pilot assignment process for the users of the target cell depends on, both the squared channel quality ω_k and the minimized outgoing interference ξ_k , which is caused by users sharing the same pilot sequence in the level V_k . The optimization problem in (17) can be solved with the help of the SPA algorithm. In this algorithm, users that suffer setbacks due to bad channel quality are exempted from the pilot sequence as it will cause severe interference. Thus, the sets of users with the worst channel quality are assigned pilot sequence with the lowest inter-cell interference. For the remaining cells, the process will continue in a sequential way, excluding the cells that are already included with the target cell.

Furthermore, our algorithm is not computationally intensive in the sense that it ultimately relies on cell sorting, thus the time complexity it incurs is $O(L K \log K)$, and therefore it works faster if compared to recent schemes. For example, EPA shows less computational complexity than the work in [19,21], which incur $O(L K^3)$ and $O(L^2 K \log K)$, respectively. In addition, the scheme in [17] incurs $O(M(K_e^2 + K_{CS}^2))$, where K_e denotes the number of edge users in the network, and K_{CS} represents the number of users in the largest cell. So apparently [17] is much more intense than EPA. The SPA scheme [11], as it is fundamentally limited to only a target cell optimization, unsurprisingly it incurs only $O(K \log K)$.

6. Simulation Results

The base code implemented is obtained from [26], while Monte Carlo simulation is used to evaluate the performance of the EPA scheme. A typical hexagonal cellular network made up of L cells is considered in the EPA scheme. Each of these cells comprises of a BS which is equipped with M number of antennas and K users with single antennas under its coverage area [2,5]. A center cell surrounded by all other cells is considered as a target cell. The system parameters are summarized in Table 1. The parameter β_{ik}^i is modeled in decibel as [10]:

$$\beta_{ik}^i = Y + 10 \alpha \log_{10} \left(\frac{d_{jk}^i}{1 \text{ km}} \right) + F_{jk}^i \tag{18}$$

where d_{jk}^i (km) is the distance between the k -th user in the j -th cell and the BS in the i -th cell, α is the path-loss exponent, Y determines the median channel gain at 1 km as a reference distance which can be calculated according to many propagation models [33], and $F_{jk}^i \sim \mathcal{N}(0, \sigma_{sf}^2)$ is the shadow fading which creates log-normal random variations around the nominal value $Y + 10 \alpha \log_{10}(d_{jk}^i/1 \text{ km})$.

Table 1. Simulation parameters.

Parameter	Value (for Figures 3–12)	Value (for Figure 13)
Number of Cells L	7	7
Number of BS Antennas M	$8 \leq M \leq 512$	$8 \leq M \leq 512$
Number of users in each cell K	8	20
Cell Radius R	500 m	300 m
Cell edge SNR	15 dB	20 dB
Path-loss Exponent α	3	3
Shadow Fading Standard Deviation σ_{sf}^2	8	8
Thermal Noise Variance	-174 dBm/H	-174 dBm/H

We evaluate the SPA [11] and the conventional schemes [2,5] against the EPA scheme. Figure 3 depicts the average uplink rate per user of the EPA, SPA and conventional schemes against the number of BS’s antennas using the ZF as a linear detector. Obviously, the average uplink rate of the EPA scheme outperforms the other schemes. This improvement can be attributed to the policy implemented for pilot assignment in the neighbor cells. This implemented policy ensures a significant reduction of the inter-cell interference at the serving BS, which invariably leads to a better throughput. Due to the pilot assignment in the target cell which was executed according to the users’ channel quality, the SPA scheme achieves better performance than the other conventional scheme. However, the performance of both SPA and conventional schemes changes slightly when the number of antennas exceeds certain points (e.g., greater than 150).

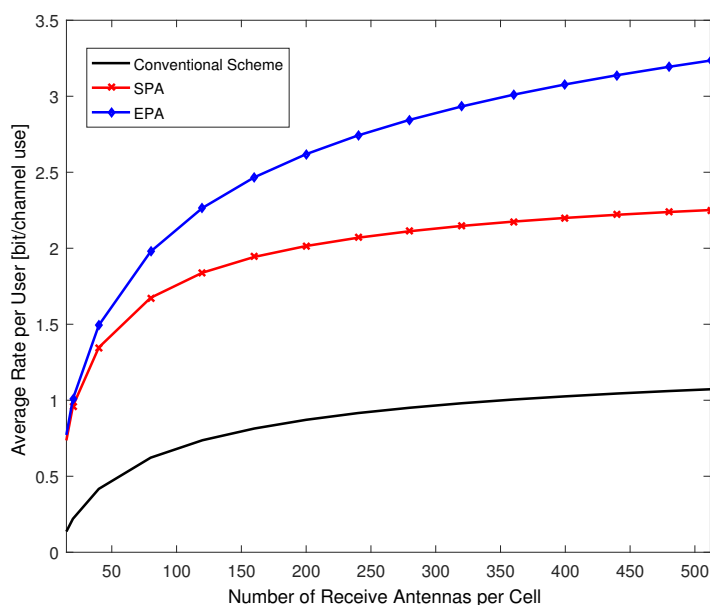


Figure 3. The average uplink rate per user with zero forcing (ZF) for different numbers of antennas.

Figure 4 shows the impact of the EPA scheme when using the MRC as a linear detector. It can be clearly observed that the average uplink rate per user (bits/channel use) is substantially enhanced by the EPA scheme when the number of antennas is increased. The superiority of the EPA scheme over other schemes, arose as a result of the minimization of the inter-cell interference that comes from the neighbor cells. This is achieved by allowing the users in each interference level V_k to share the same pilot sequence. Consequently, EPA scheme has shown a low interference from the neighbor cells compared to the other schemes.

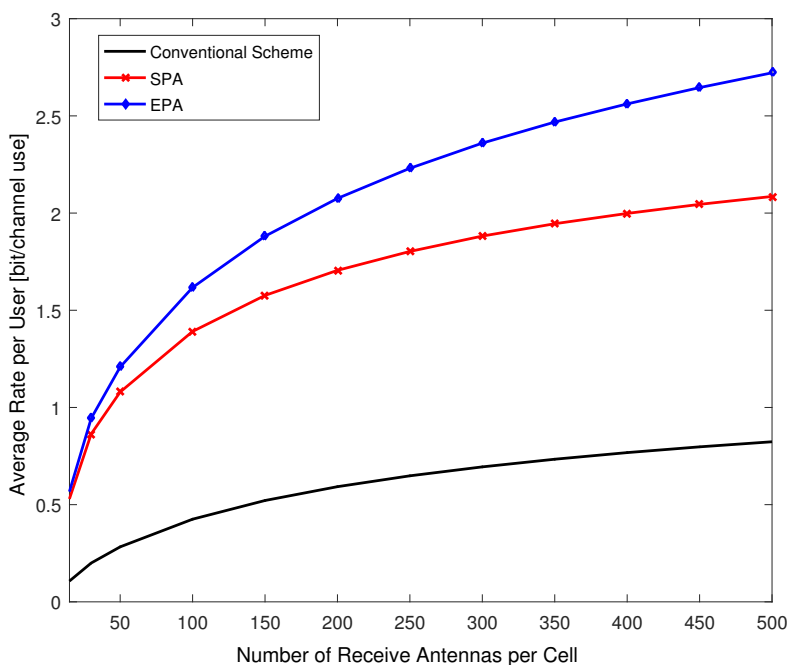


Figure 4. The average uplink rate per user with maximum ratio combining (MRC) for different numbers of antennas.

Figure 5 depicts the performance of the EPA scheme when compared with both conventional and SPA schemes in terms of cumulative distribution function (CDF) of the average SINR. When the number of BS’s antennas is 64 with ZF detector, the probabilities of the average uplink SINR being less than -10 dB for the conventional, the SPA, and the proposed EPA schemes are almost 80%, 26.25%, and 10%, respectively. The improvement is achieved because the effect of the interference, which is associated with the pilot sequences, on channel quality of the users in the target cell became slight, which effectively increased the SINR of the system.

Figure 6 depicts the CDF of the minimum SINR when M is 64. It is evident that the minimum SINR of the EPA scheme is significantly improved when compared with SPA and conventional schemes. For example, the probability of the minimum SINR to be less than -20 dB for the EPA scheme is approximately 16.25%, while this probability is about 34.6% and 79.6% for the SPA and the conventional schemes, respectively. The reason behind this improvement is due to assigning the pilots of the users with the lowest interference, in the neighbor cells, to the users who have bad channel quality in the target cell. In consequence, the performance of these users was improved due to the reduction of their interference.

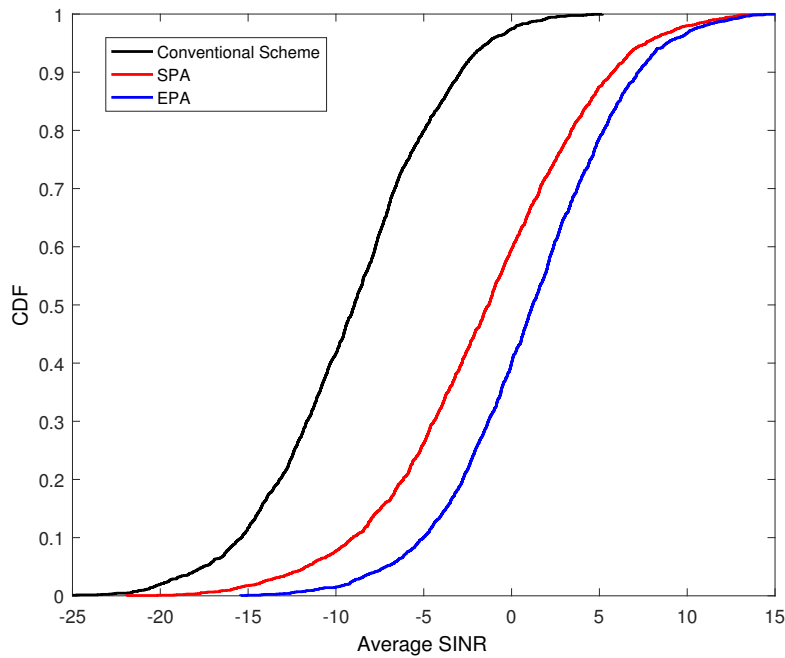


Figure 5. The cumulative distribution function (CDF) of the average signal-to-interference-plus-noise ratio (SINR) when $M = 64$ using ZF.

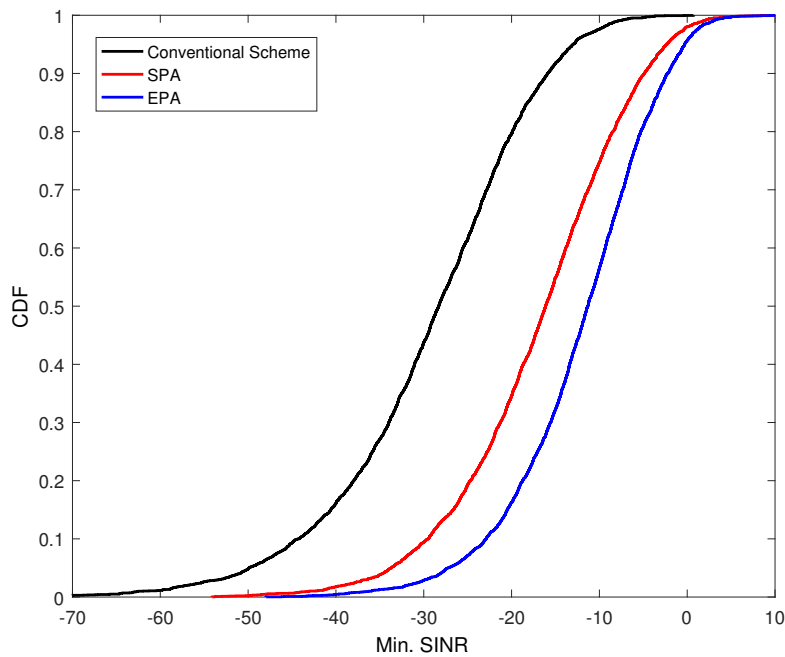


Figure 6. The CDF of the min. SINR when $M = 64$ using ZF.

Figures 7 and 8 depict the CDF of average and minimum SINR, respectively, using MRC detector when M is 64. As observed from Figures 7 and 8, the EPA scheme outperforms the SPA and the conventional

schemes. As shown in Figure 7, the EPA scheme increases the average SINR by 1.8 dB over the SPA scheme, whereas it increases up to 4.69 dB for minimum SINR, as illustrated in Figure 8.

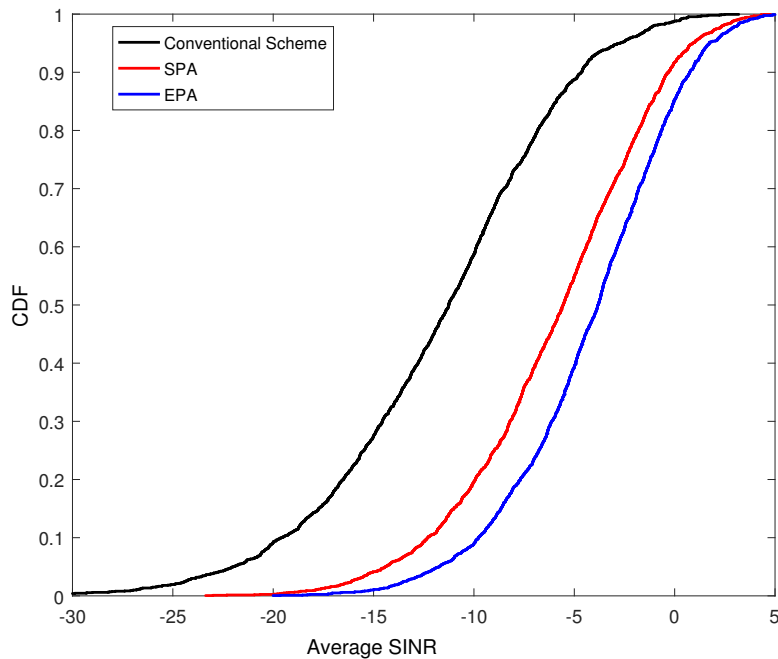


Figure 7. The CDF of the average SINR when $M = 64$ using MRC.

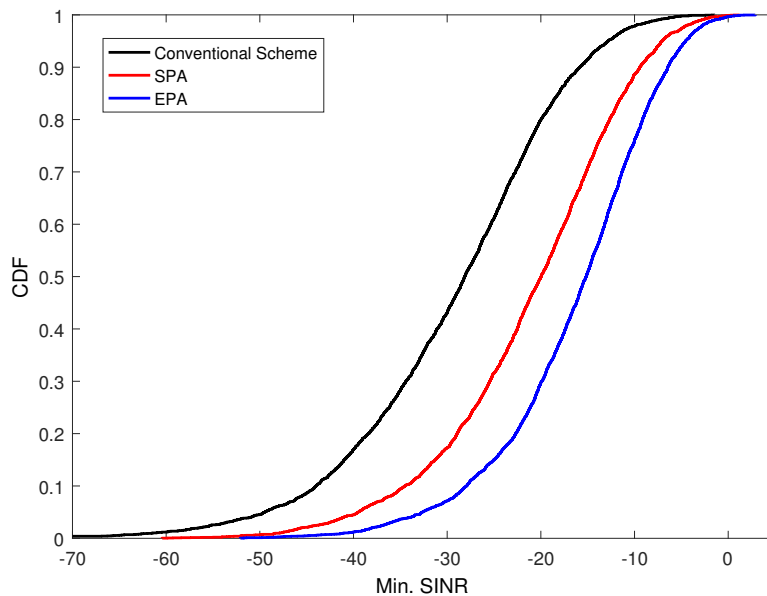


Figure 8. The CDF of the min. SINR when $M = 64$ using MRC.

From Figures 5–8, the minimum SINR always achieves a better performance. In other words, the performance of edge users is significantly enhanced. This is due to the fact that the inter-cell interference has been greatly reduced at the target cell while the users with poor channel quality are assigned to the

suitable pilot sequences in order to maximize its SINR. Moreover, the results obtained as a result of using ZF and MRC linear detections, are approximately comparable when run on the same parameters setting. This is because the inter-cell interference is greatly reduced by the EPA scheme that runs before the process of signal detection.

By using ZF detector, the performance of the EPA scheme has been examined in terms of the CDF of the average uplink rate when M is 64, as shown in Figure 9. It can be seen that the performance of the CDF in the conventional scheme is highly influenced by the pilot contamination. The assignment of the pilot randomly, has led to the worst performance compared to the SPA and the EPA schemes. On the other hand, the EPA scheme outperforms the SPA and the conventional schemes, since the effect of users who cause the highest interference is considered weak compared to users having good channel quality when they are assigned the same pilot sequence. As a result, these interfering users are excluded from sharing the same pilots of users with bad channel quality.

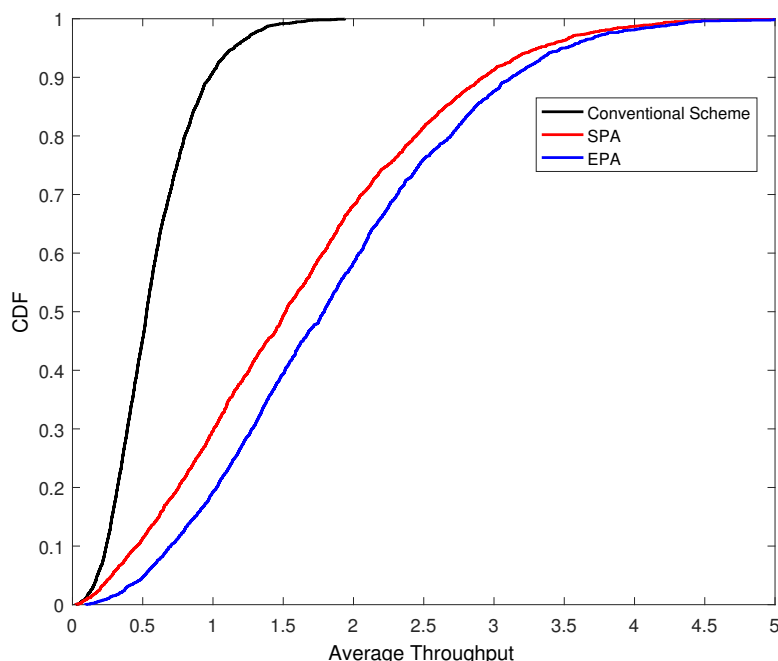


Figure 9. The CDF of the average uplink rate when $M = 64$ using ZF.

Result of evaluation for the CDF of the minimum uplink rate is depicted in Figure 10. It is clear that the EPA scheme performs better than the other schemes. For example, the minimum uplink rate of the EPA scheme is doubled when compared to the SPA scheme. This improvement has been achieved because the interference associated with pilot sequences, which is allocated to users with bad channel quality, was reduced effectively by the EPA scheme.

Figures 11 and 12 represent the CDF of the average and the minimum uplink rate, respectively, when the MRC is utilized and M is 64. The EPA scheme achieves the highest performance when compared with other schemes, especially in the minimum uplink rate. Specifically, the achieved gain in minimum uplink rate is doubled while it is 1.2 times in average uplink rate in comparison with SPA. The reason for this improvement in the minimum uplink rate is due to the priority given to the users having the worst channel quality during the pilot assignment process.

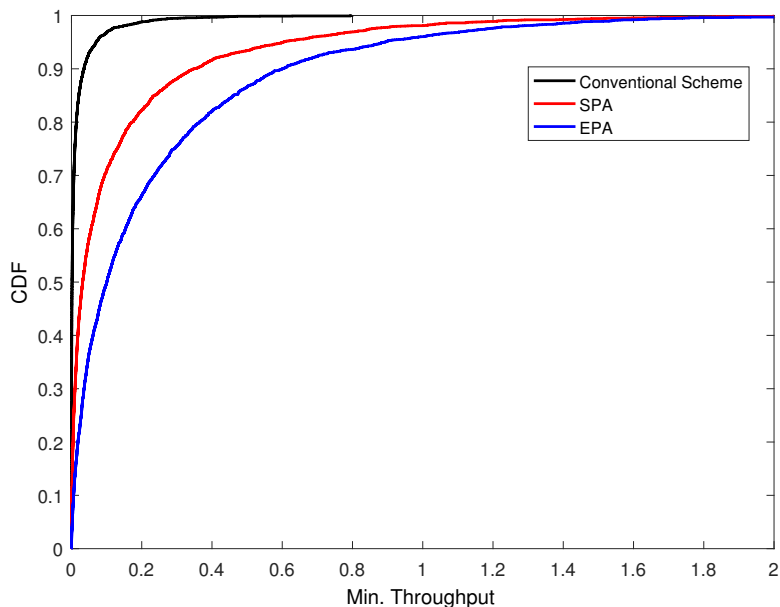


Figure 10. The CDF of min. uplink rate when $M = 64$ using ZF.

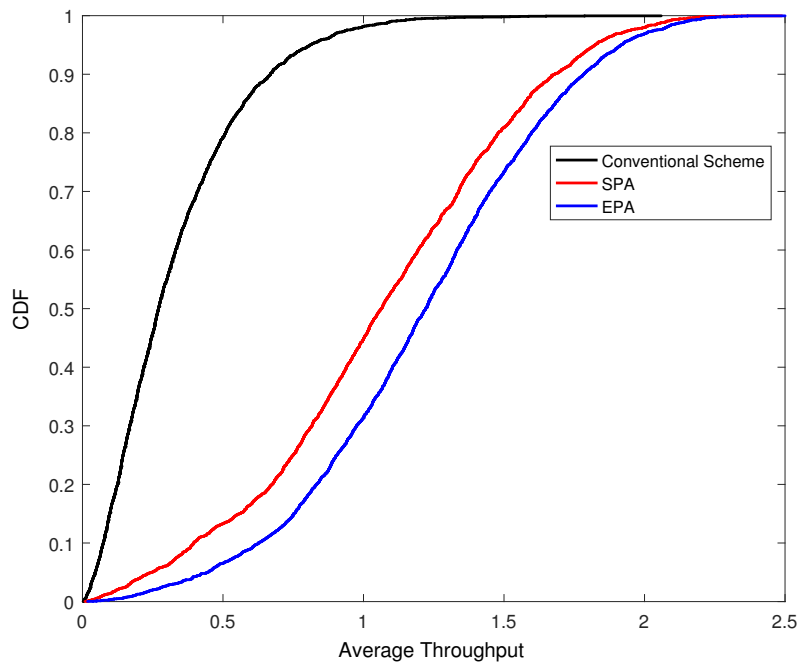


Figure 11. The CDF of average uplink rate when $M = 64$ using MRC.

In order to verify the effectiveness of the EPA scheme, the average uplink rate against the number of antennas has been evaluated in Figure 13 with different parameters, considering ZF detector. These parameters, which are shown in Table 1, increase the interference severity at the target cell. Obviously, the average uplink rate of EPA schema is higher than other schemes, despite the intensity of interference.

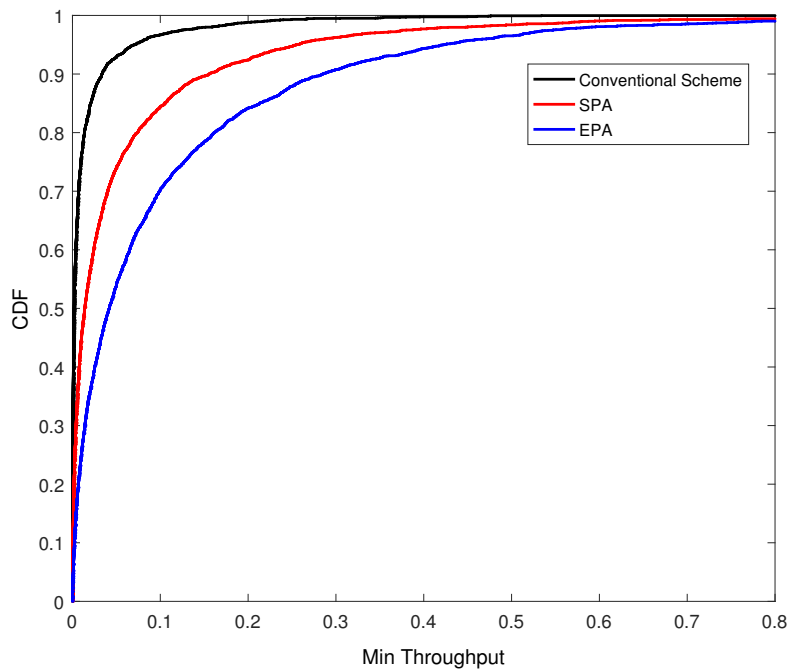


Figure 12. The CDF of min. uplink rate when $M = 64$ using MRC.

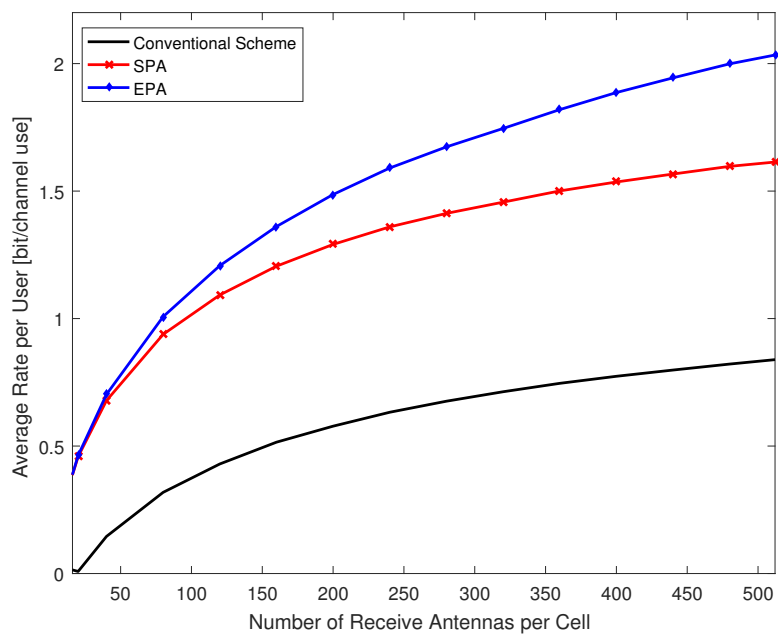


Figure 13. The average uplink rate per user with ZF for different numbers of antennas, $K = 20$, and $R = 300$ m.

7. Conclusions

In this paper, we propose a new pilot assignment approach to address the pilot contamination in multicell massive MIMO systems. An optimization problem is formulated in order to improve the minimum uplink rate for users in the target cell. Our approach to solving this optimization problem ensures an overall reduction of the outgoing inter-cell interference of neighbor cells. This reduction is achieved by assigning the pilot sequences to the neighbor cell's users and maximizing the minimum uplink rate of the target cell's users based on SPA algorithm. The numerical results have clearly shown that the EPA scheme is more effective than the other schemes in both MRC and ZF linear detections. Additionally, using such an efficient assigning approach entitles the new EPA scheme to achieve significant performance when the typical parameter M is 64 compared to the SPA and the conventional schemes. Likewise, the minimum uplink rate is greatly enhanced by the new EPA scheme than the SPA scheme. Furthermore, the proposed scheme has also proved high effectiveness and performance even in severe interference environments.

Author Contributions: Conceptualization, A.S.A.-h. and N.K.N.; Formal analysis, A.S.A.-h. and N.K.N.; Methodology, A.S.A.-h., N.K.N., A.S., S.S. and A.M.M.; Writing—review & editing, A.S.A.-h. and N.K.N.

Funding: This work was funded by [Advancing the State of the Art of MIMO: The Key to Successful Evolution of Wireless Networks (ATOM)] grant number [690750-ATOM-H2020-MSCA- RISE-2015, UPM: 6388800-10801] and The APC was funded by [Research Management Centre (RMC)].

Conflicts of Interest: The authors declare no conflicts of interest.

References

1. Boccardi, F.; Heath, R.W.; Lozano, A.; Marzetta, T.L.; Popovski, P. Five disruptive technology directions for 5G. *IEEE Commun. Mag.* **2014**, *52*, 74–80. [[CrossRef](#)]
2. Marzetta, T.L. Noncooperative cellular wireless with unlimited numbers of base station antennas. *IEEE Trans. Wirel. Commun.* **2010**, *9*, 3590–3600. [[CrossRef](#)]
3. Lim, Y.G.; Chae, C.B.; Caire, G. Performance analysis of massive MIMO for cell-boundary users. *IEEE Trans. Wirel. Commun.* **2015**, *14*, 6827–6842. [[CrossRef](#)]
4. Larsson, E.G.; Edfors, O.; Tufvesson, F.; Marzetta, T.L. Massive MIMO for next generation wireless systems. *IEEE Commun. Mag.* **2014**, *52*, 186–195. [[CrossRef](#)]
5. Rusek, F.; Persson, D.; Lau, B.K.; Larsson, E.G.; Marzetta, T.L.; Edfors, O.; Tufvesson, F. Scaling up MIMO: Opportunities and challenges with very large arrays. *IEEE Signal Process. Mag.* **2013**, *30*, 40–60. [[CrossRef](#)]
6. Björnson, E.; Larsson, E.G.; Debbah, M. Optimizing multi-cell massive MIMO for spectral efficiency: How many users should be scheduled? In Proceedings of the 2014 IEEE Global Conference on Signal and Information Processing (GlobalSIP), Atlanta, GA, USA, 3–5 December 2014. [[CrossRef](#)]
7. Rajatheva, N.; Osseiran, A.; Monserrat, J.F.; Marsch, P. *5G Mobile and Wireless Communications Technology*; Osseiran, A., Monserrat, J.F., Marsch, P., Eds.; Cambridge University Press: Cambridge, UK, 2016; ISBN 978-1-107-13009-8.
8. Björnson, E.; Larsson, E.G.; Marzetta, T.L. Massive MIMO: Ten myths and one critical question. *IEEE Commun. Mag.* **2016**, *54*, 114–123. [[CrossRef](#)]
9. Jose, J.; Ashikhmin, A.; Marzetta, T.; Vishwanath, S. Pilot Contamination and Precoding in Multi-Cell TDD Systems. *IEEE Trans. Wirel. Commun.* **2011**, *10*, 2640–2651. [[CrossRef](#)]
10. Björnson, E.; Hoydis, J.; Sanguinetti, L. Massive MIMO Networks: Spectral, Energy, and Hardware Efficiency. *Found. Trends Signal Process.* **2017**, *11*, 154–655. [[CrossRef](#)]
11. Zhu, X.; Wang, Z.; Dai, L.; Qian, C. Smart Pilot Assignment for Massive MIMO. *IEEE Commun. Lett.* **2015**, *19*, 1644–1647. [[CrossRef](#)]

12. Dao, H.T.; Kim, S. Vertex Graph-Coloring-Based Pilot Assignment With Location-Based Channel Estimation for Massive MIMO Systems. *IEEE Access* **2018**, *6*, 4599–4607. [[CrossRef](#)]
13. Kim, K.; Lee, J.; Choi, J. Deep Learning Based Pilot Allocation Scheme (DL-PAS) for 5G Massive MIMO System. *IEEE Commun. Lett.* **2018**, *22*, 828–831. [[CrossRef](#)]
14. Akbar, N.; Yan, S.; Yang, N.; Yuan, J. Location-Aware Pilot Allocation in Multicell Multiuser Massive MIMO Networks. *IEEE Trans. Veh. Technol.* **2018**, *67*, 7774–7778. [[CrossRef](#)]
15. Muppirisetty, L.S.; Charalambous, T.; Karout, J.; Fodor, G.; Wymeersch, H. Location-Aided Pilot Contamination Avoidance for Massive MIMO Systems. *IEEE Trans. Wirel. Commun.* **2018**, *17*, 2662–2674. [[CrossRef](#)]
16. Sohn, J.; Yoon, S.W.; Moon, J. On Reusing Pilots Among Interfering Cells in Massive MIMO. *IEEE Trans. Wirel. Commun.* **2017**, *16*, 8092–8104. [[CrossRef](#)]
17. Zhu, X.; Wang, Z.; Qian, C.; Dai, L.; Chen, J.; Chen, S.; Hanzo, L. Soft Pilot Reuse and Multi-Cell Block Diagonalization Precoding for Massive MIMO Systems. *IEEE Trans. Veh. Technol.* **2016**, *65*, 3285–3298. [[CrossRef](#)]
18. ZLiu, J.; Li, Y.; Zhang, H.; Guo, S. Efficient and Fair Pilot Allocation for Multi-cell Massive MIMO Systems. In Proceedings of the 2017 9th International Conference on Wireless Communications and Signal Processing (WCSP), Nanjing, China, 11–13 October 2017. [[CrossRef](#)]
19. Ma, S.; Xu, E.L.; Salimi, A.; Cui, S. A Novel Pilot Assignment Scheme in Massive MIMO Networks. *IEEE Commun. Lett.* **2018**, *7*, 262–265. [[CrossRef](#)]
20. Wang, H.; Huang, Y.; Jin, S.; Du, Y.; Yang, L. Pilot Contamination Reduction in Multi-cell TDD Systems with Very Large MIMO Arrays. *Wirel. Pers. Commun.* **2017**, *96*, 5785–5808. [[CrossRef](#)]
21. Du, T.; Wang, Y.; Wang, J.; Du, Y.; Yang, L. Multi-cell Joint Optimization to Mitigate Pilot Contamination for Multi-Cell Massive MIMO Systems. In Proceedings of the 2017 IEEE 85th Vehicular Technology Conference (VTC Spring), Sydney, NSW, Australia, 4–7 June 2017. [[CrossRef](#)]
22. Wang, P.; Zhao, C.; Zhang, Y.; Stuber, G.L. A Novel Pilot Assignment Approach for Pilot Decontaminating in Massive MIMO Systems. In Proceedings of the 2017 IEEE Wireless Communications and Networking Conference (WCNC), San Francisco, CA, USA, 19–22 March 2017. [[CrossRef](#)]
23. Zhao, M.; Zhang, H.; Guo, S.; Yuan, D. Joint Pilot Assignment and Pilot Contamination Precoding Design for Massive MIMO Systems. In Proceedings of the 2017 26th Wireless and Optical Communication Conference (WOCC), Newark, NJ, USA, 7–8 April 2017. [[CrossRef](#)]
24. Fernandes, F.; Ashikhmin, A.; Marzetta, T.L. Inter-Cell Interference in Noncooperative TDD Large Scale Antenna Systems. *IEEE J. Sel. Areas Commun.* **2013**, *31*, 192–201. [[CrossRef](#)]
25. Chen Z.; Yang, C. Pilot decontamination in wideband massive MIMO systems by exploiting channel sparsity. *IEEE Trans. Wirel. Commun.* **2016**, *15*, 5087–5100. [[CrossRef](#)]
26. Björnson, E.; Matthaiou, M.; Debbah, M. Massive MIMO with Non-Ideal Arbitrary Arrays: Hardware Scaling Laws and Circuit-Aware Design. *IEEE Trans. Wirel. Commun.* **2015**, *14*, 4353–4368. [[CrossRef](#)]
27. Li, M.; Jin, S.; Gao, X. Spatial Orthogonality-Based Pilot Reuse for Multi-cell Massive MIMO Transmission. In Proceedings of the 2013 International Conference on Wireless Communications and Signal Processing, Hangzhou, China, 24–26 October 2013. [[CrossRef](#)]
28. Ashikhmin, A.; Marzetta, T. Pilot Contamination Precoding in Multi-Cell Large Scale Antenna Systems. In Proceedings of the 2012 IEEE International Symposium on Information Theory Proceedings, Cambridge, MA, USA, 1–6 July 2012. [[CrossRef](#)]
29. Muller, R.; Cottatellucci, L.; Vehkaperä, M. Blind pilot decontamination. *IEEE J. Sel. Top. Signal Process.* **2014**, *8*, 773–786. [[CrossRef](#)]
30. Ngo, H.Q.; Larsson, E.G.; Marzetta, T.L. Energy and Spectral Efficiency of Very Large Multiuser. *IEEE Trans. Wirel. Commun.* **2013**, *61*, 1436–1449. [[CrossRef](#)]
31. Sesia, S.; Toufik, I.; Baker, M. Network Architecture and Protocols. In *LTE-The UMTS Long Term Evolution: From Theory to Practice*; John Wiley & Sons Ltd.: Chichester, UK, 2011; ISBN 978-0-470-66025-6.

32. Zhu, X.; Dai, L.; Wang, Z. Graph coloring based pilot allocation to mitigate pilot contamination for multi-cell massive mimo systems. *IEEE Commun. Lett.* **2015**, *19*, 1842–1845. [[CrossRef](#)]
33. Sarkar, T.K.; Ji, Z.; Kim, K.; Medouri, K.; Salazar-Palma, M. A survey of various propagation models for mobile communication. *IEEE Antennas Propag. Mag.* **2003**, *45*, 51–82. [[CrossRef](#)]



© 2019 by the authors. Licensee MDPI, Basel, Switzerland. This article is an open access article distributed under the terms and conditions of the Creative Commons Attribution (CC BY) license (<http://creativecommons.org/licenses/by/4.0/>).